Chinese Chemical Letters 35 (2024) 108687

Contents lists available at ScienceDirect

Chinese Chemical Letters

journal homepage: www.elsevier.com/locate/cclet

Passive daytime radiative cooling coatings with renewable self-cleaning functions

Qian Wu[a], Yubo Cui[a,b], Guifeng Xia[a,b], Jinlong Yang[a], Shuming Du[c], Xinhong Xiong[b], Li Yang[d], Dong Xu[c], Xu Deng[a], Jiaxi Cui[a,b,*]

[a] Institute of Fundamental and Frontier Sciences, University of Electronic Science and Technology of China, Chengdu 610054, China
[b] Yangtze Delta Region Institute (Huzhou), University of Electronic Science and Technology of China, Huzhou 313001, China
[c] Beijing Key Laboratory of Power Generation System Functional Material, CHN Energy New Energy Technology Research Institute Ltd., Beijing 102209, China
[d] Institute for Advanced Study, Chengdu University, Chengdu 610106, China

ARTICLE INFO

Article history:
Received 3 April 2023
Revised 8 June 2023
Accepted 11 June 2023
Available online 15 June 2023

Keywords:
Superhydrophobic
Passive radiative cooling
Wearing
Regeneration
Glass resin armor

ABSTRACT

Passive daytime radiative cooling (PDRC) technology is emerging as one of the most promising solutions to the global problem of spacing cooling, but its practical application is limited due to reduced cooling effectiveness caused by daily wear and tear, as well as dirt contamination. To tackle this problem, we report a novel strategy by introducing a renewable armor structure for prolonging the anti-fouling and cooling effectiveness properties of the PDRC coatings. The armor structure is designed by decorating fluorinated hollow glass microspheres (HGM) inside rigid resin composite matrices. The HGM serve triple purposes, including providing isolated cavities for enhanced solar reflectance, reinforcing the matrices to form robust armored structures, and increasing thermal emittance. When the coatings are worn, the HGM on the surface expose their concave cavities with numerous hydrophobic fragments, generating a highly rough surface that guarantee the superhydrophobic function. The coatings show a high sunlight reflectance (0.93) and thermal emittance (0.94) in the long-wave infrared window, leading to a cooling of 5 °C below ambient temperature under high solar flux (~900 W/m^2). When anti-fouling functions are reduced, they can be regenerated more than 100 cycles without compromising the PDRC function by simple wearing treatment. Furthermore, these coatings can be easily prepared using a one-pot spray method with low-cost materials, exhibit strong adhesion to a variety of substrates, and demonstrate exceptional environmental stability. Therefore, we anticipate their immediate application opportunities for spacing cooling.

Space cooling has become a global concern as it consumes 15% of global electricity and yields 10% greenhouse gas emissions [1]. Many measures are being pursued to address this issue, and one of the most promising approaches is passive daytime radiative cooling (PDRC) technology. This green technology is usually based on coatings that reflect sunlight in the wavelength range of 0.3–2.5 μm and radiate heat to the cold outer space through the atmosphere's long-wave infrared (LWIR) transmission window (wavelength range of 8–13 μm) [2–12]. Recently, such a combination has been achieved in cheap and scalable polymer paints by introducing cavities or particles into coating matrices to induce light scattering [4,9,13-18]. These coatings show excellent spectroscopic results, but their practical applications are still rare. It is mainly due to their poor longevity in PDRC function as a consequence of solid contaminants (dust or other microparticles) or daily wear and tear. Solid contaminants will quickly accumulate on coatings surfaces to decrease the sunlight reflectance and thermal-infrared emission [19], while inevitable daily wear and tear would damage the delicate structures. Besides longevity, weak mechanical properties, low adhesion on substrates, and poor water-repellency may also constitute the determinate reasons for disenabling the practical use of these materials. Therefore, it is still desirable to develop robust PDRC coatings with a mechanism to prevent contamination.

Lotus leaf-like superhydrophobicity represents one of the most powerful self-cleaning strategies [20–22]. Recently, it has been integrated into PDRC coatings for elongating surface cooling performance. Two strategies have been developed to this end, including covering superhydrophobic structures/layers on PDRC coatings [23–25] or utilizing the intrinsic porous/heterogeneous nature of PDRC coatings to create rough surfaces [26–32]. The former frequently

* Corresponding author.
E-mail address: jiaxi.cui@uestc.edu.cn (J. Cui).

https://doi.org/10.1016/j.cclet.2023.108687
1001-8417/

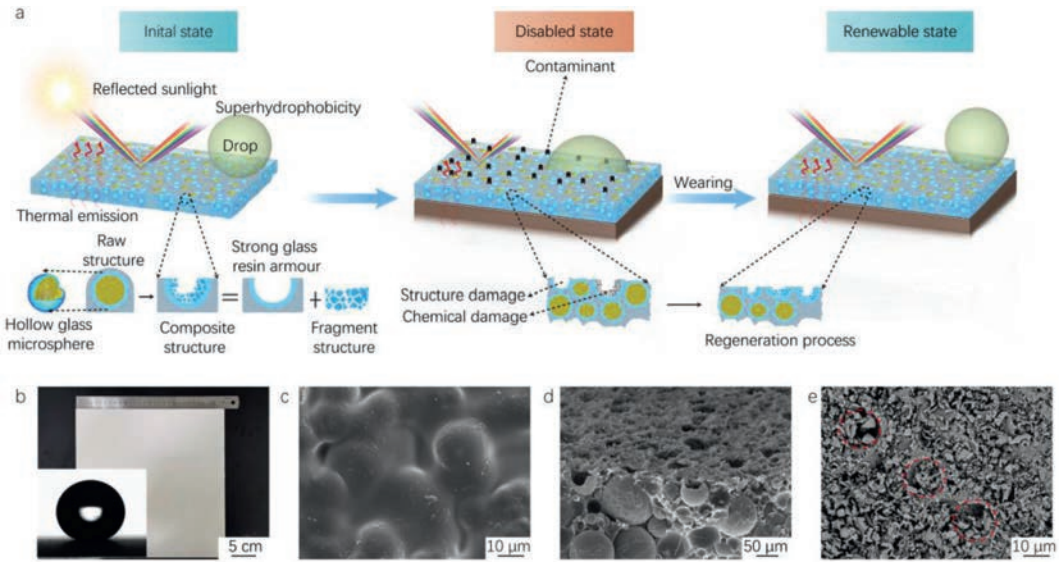

Fig. 1. Design and preparation of HGM-FHA coatings. (a) Diagrammatic representation of the design concept for the HGM-FHA coatings. (b) Photograph of a HGM-FHA coating on a 30 cm × 30 cm glass plate (inset, water contact angle image). (c) SEM image of the surface of a raw coating. SEM vertical cross-section (d) and surface (e) images of a HGM-FHA coating. All HGM-FHA coatings contain 80 wt% HGM and have an average HGM size of ~8 μm.

involves complicated fabrication and interfacial issues due to the bilayer structures. Introducing new layers/components would also reduce the PDRC function due to their sunlight absorption or low sunlight reflectance. In contrast, the latter mainly depend on the porous structures that provide PDRC matrices and superhydrophobic rough surfaces. Although this class of coatings can be prepared by facile one-pot methods, the balance of two functions often leads to compromise in cooling performance. Moreover, only modest robustness in superhydrophobicity can be achieved in these systems. Since preparing superhydrophobic surfaces mechanically robust enough for practical use is already an endless task for materials scientists, it is challenging to design PDRC coatings combining excellent radiative cooling effect and robust superhydrophobicity without tradeoffs in other performance of a paint required for practical applications.

Herein, we propose an alternative strategy to address this issue. Rather than preventing mechanical wearing, we utilize this inevitable phenomenon to renew superhydrophobicity. Fig. 1a shows our design to realize this concept. The polymer-composite coatings consist of hollow glass microspheres (HGM) and resins. HGM are introduced for three purposes, *i.e.*, providing isolated cavities to induce sunlight reflectance, reinforcing the coatings, and forming wearing-renewed rough surfaces. Sunlight reflectance occurs on interfaces generated by media with different reflection indices (RI). Although both cavities and particles can induce such heterogeneities, cavities could be the preferable option because of two reasons: (1) The RI difference between air and solid matrices is large (0.4–0.5) in comparison to typical particle-based coatings (0.1–0.2, such as typical $BaSO_4$-acylate paints); (2) Cavities would not show any absorption of sunlight while particles fillers (*e.g.*, TiO_2) typically exhibit weak absorption. This advantage has been proved by highly porous polymer systems [11]. However, high cavity content would make the substrates brittle or fluffy. In contrast, the use of HGM not only allows for tunable porosity but would also reinforce the coatings because of their rigid nature. More importantly, the structures of HGM-containing composites allow for (re)generation of superhydrophobic surfaces with enhanced sunlight reflectance performance when daily wear and tear occurs. Briefly, the composite coatings are typically robust. After severe abrasion strong enough to remove the resin, the HGM fixed in the resin would be broken to reveal their highly concave cavities and form strong glass armor. The fragments generated in the wearing would deposit into the cavities, creating highly rough surfaces. The surfaces would also provide more interfaces for sunlight reflectance. With this design, we get a high sunlight reflectance of 0.93 and a high emittance of 0.94 at the LWIR window as well as renewable, robust superhydrophobicity. The coatings can be prepared by one-pot spray from cheap materials, showing good adhesion to various substrates (3 MPa), high compression strength (26 MPa), and excellent environmental stability.

Fluorinated hydroxy acrylic resin (FHA, one of the most common resins used for paints, see Experimental Section 3.1 and Table S1 in Supporting information for their synthesis and characterization) were selected as polymer matrices because of their excellent adhesion and hydrophobic nature (Fig. S1 in Supporting information). HGM were modified with perfluoroalkyl chains to provide hydrophobic surfaces (Fig. S2 and Experimental Section 3.2 in Supporting information). The mixture of FHA, HGM, curing agent, and solvent in a mass ratio of 1:4:0.2:11 was used as the typical precursor suspension to show our idea. This suspension could be coated on various substrates *via* facile spraying, rolling, or brushing (Movie S1 in Supporting information). After drying in air for 2 d, raw HGM-FHA coatings were obtained. A scraper was used in our case to control the thickness of the coatings for study, and sandpapers were employed to wear the raw coatings to (re)generate superhydrophobic surfaces (Fig. S3 in Supporting information). This simple method allowed us to prepare large coatings on different substrates, such as a 30 cm × 30 cm coating on glass (Fig. 1b).

We monitored the forming process of the rough structures using scanning electron microscopy (SEM). As shown in Fig. 1c, the raw coatings display moderately rough surfaces made from polymer-covered HGM. The surfaces were hydrophobic, showing a water contact angle (WCA) of 116° and a water rolling angle (WRA) of >20°. Sandpaper-wearing treatment would break the HGM on the surfaces, exposing their hollow structures (Fig. 1d). Fine fragments were observed in the concave cavities (Fig. 1e). These fragments felled with the hydrophobic side up (Fig. S4 in Supporting information). As a result of such highly rough structures, the surfaces display a high WCA of 154° and a low WRA of 3°, indicating superhydrophobicity. The coatings also exhibit exceptional dynamic wettability, as evidenced by the complete bouncing off of water

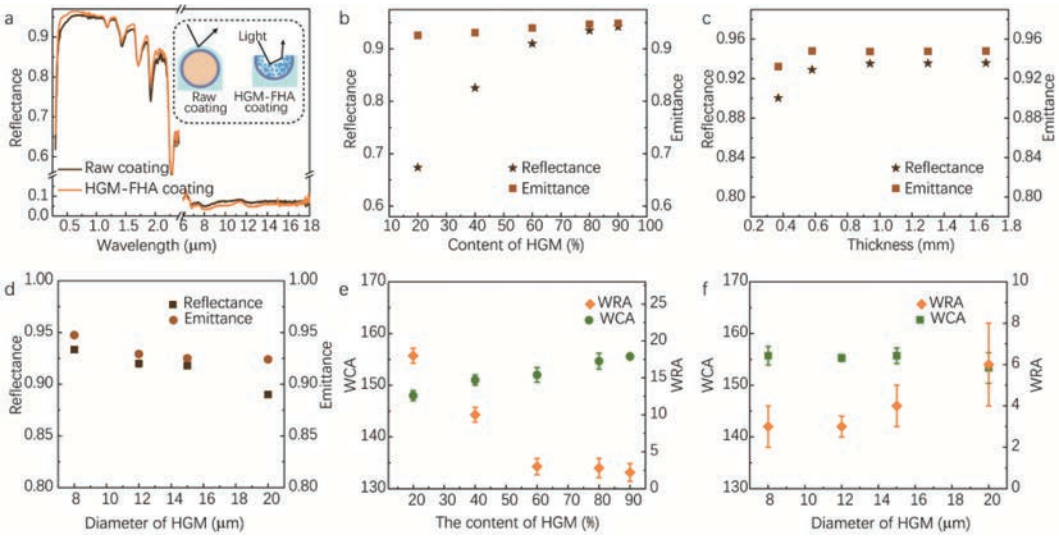

Fig. 2. Characterization of the HGM-FHA coatings. (a) Measured reflectance spectra of the HGM-FHA coatings with 80 wt% HGM (average HGM size of ~8 μm) from the ultraviolet to the mid-infrared (Inset, comparison of the light scattering behavior between raw coatings and HGM-FHA coatings). (b) Average reflectance and emittance of the HGM-FHA coatings with different HGM (average HGM size of ~8 μm) mass fractions. All the coatings have thicknesses of 0.8 mm. (c) Reflectance and emittance of HGM-FHA coatings with different thicknesses. The samples contain 80 wt% HGM with an average size of ~8 μm. (d) The optical properties of the HGM-FHA coatings with different diameters of HGM. The samples contain 80 wt% HGM and have thicknesses of 0.8 mm. (e) The wetting properties of the HGM-FHA coatings with different HGM (average HGM size of ~8 μm) mass fractions. (f) The wetting properties of the HGM-FHA coatings with different diameters of HGM. The samples contain 80 wt% HGM and have thicknesses of 0.8 mm.

droplets from the surface captured by a high-speed video camera (Fig. S5 and Movie S2 in Supporting information).

With the coatings in our hands, we first evaluated their optical properties. Fig. 2a shows the typical reflection of the HGM-FHA coatings (80% HGM mass fraction) in the sunlight spectrum (0.3–2.5 μm) and LWIR transmission window (8–13 μm). The typical samples contained spherical HGM with an average size of ~8 μm and a wide distribution (1.44, Fig. S6 in Supporting information). They provided a broad-spectrum scattering efficiency across the entire solar wavelengths due to the high-order Mie resonance excitations, which resulted in a high reflection of sunlight (~93% for a 0.8-mm-thick film).

Interestingly, the wearing treatment enhanced the reflection of sunlight (1% higher). It was attributed to the extra light scattering induced by these fine fragments in the concaves created by wear (inset in Fig. 2a). The sample also possessed a nearly saturated emissivity of >0.94 in the LWIR transmission window. We had employed attenuated total reflectance-Fourier transform infrared spectroscopy (ATR-FTIR) to study the absorption of the pristine materials and composite coatings in the LWIR transmission window. The composite coatings exhibit strong emittances in the atmospheric transparency window due to the stretching vibrations of Si-O-Si (HGM) and C-O-C (FHA) bonds (Fig. S7 in Supporting information). Furthermore, the HGM were mainly composed of alkali lime borosilicate with inherent absorption at the phonon-polariton resonance wavelength of 9.7 μm. As a result of these absorption, the obtained hybrid coating showed highly broadband near-normal emissions across the LWIR transparency window.

The optical properties of the composite coatings were influenced by different factors, including the fraction of HGM in the coatings, coating thickness, HGM sizes, and the type of polymers used. As shown in Fig. 2b and Fig. S8a (Supporting information), increasing HGM fraction promotes sunlight reflection, while only a minor enhancement in emissivity in the LWIR window is observed. It was because HGM determined the system's porosity. Besides HGM fraction, increasing coating thickness also favors sunlight reflection and thermal emittance in the range of 8–13 μm until a value of >0.6 mm (Fig. 2c and Fig. S8b in Supporting information). To investigate the influence of HGM sizes, we fabricated a series of composite coatings using HGM with average sizes ranging from 8 μm to 20 μm and compared their optical properties (Fig. S6). The sunlight reflectance of these coatings drops with increasing the HGM size (Fig. 2d and Fig. S9 in Supporting information). In our system, the sunlight was reflected mainly *via* Mie scattering. Increasing particle sizes beyond the sunlight wavelength would reduce the reflection [33,34]. In contrast to these changes, tested three polymer matrices display similar sunlight reflectance and thermal emittance (Fig. S10 in Supporting information). We theoretically analyzed the relationship between sunlight reflectance and cooling power [3] by setting the average thermal emittance as $E = 0.94$. It was found that the coatings could achieve a passive cooling effect when the average sunlight reflectance of the HGM-FHA coatings was greater than 0.9 (Fig. S11 in Supporting information).

We then investigated the surface properties of these coatings with different structure parameters. At first, the surface roughness of the raw coatings increases with the HGM content (Fig. S12 Supporting information). These surfaces were not superhydrophobic yet until treated by wear in the case of >40% HGM were used (Fig. 2e). We also change the HGM size to get different roughness surfaces (Fig. S13 in Supporting information). Larger HGM size would lead to slightly lower WCA and higher WRA (Fig. 2f). The sandpaper mesh was critical for forming surface micro/nanostructures when these coatings were treated with sandpaper. Large mesh favored the formation of small fragments and thus high WCA. In particular, sandpaper with a mesh of >120 was required to get stable superhydrophobicity (Fig. S14 in Supporting information). Furthermore, we conducted washing experiment to prove the stability of these fragments (Fig. S15 in Supporting information). It was found that the surface maintained its superhydrophobicity for 10-min washing. We attributed to the small size of the cavities in the broken glass sphere which stored the fragments, and the fragments surface contained the low-surface-energy fluorinated polymer leading to the extremely low adhesion of the fragments to water droplets when in contact.

In our design, rigid polymer matrices were used to ensure the occurrence of wearing-induced fracture. The obtained coatings show a high compression modulus of 26 MPa (Fig. S16 in Sup-

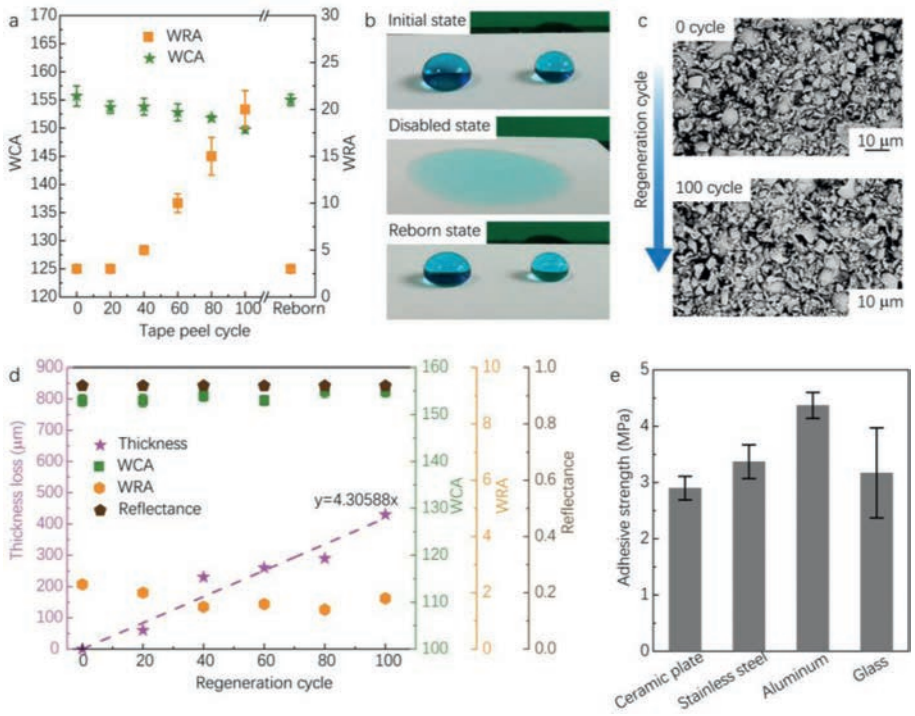

Fig. 3. Regeneration and mechanical properties of the HGM-FHA coatings. (a) Structure damage and regeneration: WCA and WRA of HGM-FHA coatings treated with 3M tape. (b) Chemical damage and regeneration: The photo of water drops on a sample at different states. (c) SEM images of a HGM-FHA coating before and after wearing treatment (100 regeneration cycles). (d) WCA, WRA, thickness and reflectance values of HGM-FHA coatings with regeneration cycle. (e) Adhesion strength of the HGM-FHA coatings on different kinds of substrate. The data were obtained by PosiTest Pull-off adhesion testing. All HGM-FHA coatings contain 80 wt% HGM and have an average HGM size of ~8 μm.

porting information). The rigid shell of HGM, serving as a skeleton structure, significantly increased the compression strength of the material, making it resistant to abrasion and able to withstand external forces without collapsing. Furthermore, the rigid nature of the matrices was expected to favor energy absorption for HGM fragmentation. To confirm this hypothesis, we replaced the stiff polymers with elastic silicone, *i.e.*, the copolymer of polydimethylsiloxane and urea (uPDMS), to prepare the HGM-uPDMS composite coatings (Fig. S17a in Supporting information). Under the same wearing treatment, no HGM were broken since the elastic matrices could dissipate the shearing force by deformation. As a result of the absence of the fragment-based nanostructure, the HGM-uPDMS coatings only reached a WCA of 148°, and their surfaces were even sticky to water droplets. We also found that using simple hydrophobic polymers as matrices might lead to other issues, such as low adhesion to the substrates. For example, polyvinylidene fluoride (PVDF) is a typical low-surface energy polymer often used to design PDRC coatings. It usually shows poor adhesion to the substrates. We prepared an HGM-PVDF composite coating to confirm this idea. Both the as-prepared and wearing-treated composite coatings were superhydrophobic. However, the adhesion of the coating was so weak that it directly peeled off from the glass substrate during drying (Fig. S17b in Supporting information). Such poor adhesion would significantly limit its application as a coating. Based on these studies, the HGM-FHA coatings with 80% HGM (average HGM size of ~8 μm) mass fraction were selected as optimized samples for further investigation.

Surface superhydrophobicity would be inevitably reduced in daily use, resulting in a remarkable decrease in the cooling effect of PDRC coatings. In our design, we proposed to utilize daily wearing to regenerate the self-cleaning function of the coatings. To probe the regeneration ability, we subjectively destroyed the structure of the HGM-FHA coatings by 3M tape peeling treatment. Briefly, a 3M tape was pasted on the coatings and peeled. It was found that the coatings were robust to suffer 40 peeling cycles without significant reduction in surface superhydrophobicity (low WRA). An evident increase in WRA occurred after 60 cycles of peeling (Fig. 3a). Such decline was attributed to the removal of fragments (Fig. S18 in Supporting information), indicating the importance of fragments in surface properties. Besides structure damage, we also evaluated the deterioration of surface chemistry on coatings properties, using plasma to change surface chemistry. After 5 min irradiation, the coatings would change from superhydrophobic to hydrophilic (Fig. 3b). The failure coatings could recover their surface properties by a simple sandpaper-wearing treatment (Movie S3 in Supporting information). In the treatment, the rigid polymer matrices were worn to expose the embedded HGM, which were then broken to regenerate the similar fragment-containing rough structure. As a demo of the regeneration process, we took a HGM-FHA coating with a thickness of 1.5 mm on a glass (2.5 cm × 2.5 cm) as an example. A weight of 100 g was attached to the back face of the sample with tape to form the test specimen. The coating surface was placed facing downwards on standard 800 mesh sandpaper and the test specimen was moved a distance of 3 cm for one regeneration cycle (Fig. S19 in Supporting information). After 100 regeneration cycles, the coating still retained its micro-nanostructure surface (Fig. 3c). We plotted the regeneration cycle with the thickness of the coating as well as the WCA, WRC, and reflectance (Fig. 3d). The coating thickness decreases with the regeneration cycle (4.3 μm/cycle). However, no apparent change occurs in either surface or optical properties. Based on the thickness-reflectance result (Fig. 2c), we did not expect any change in optical properties until the coating thickness was reduced to <600 μm.

We systematically evaluated the practical applicability of our coatings by testing their adhesion stability with various substrates

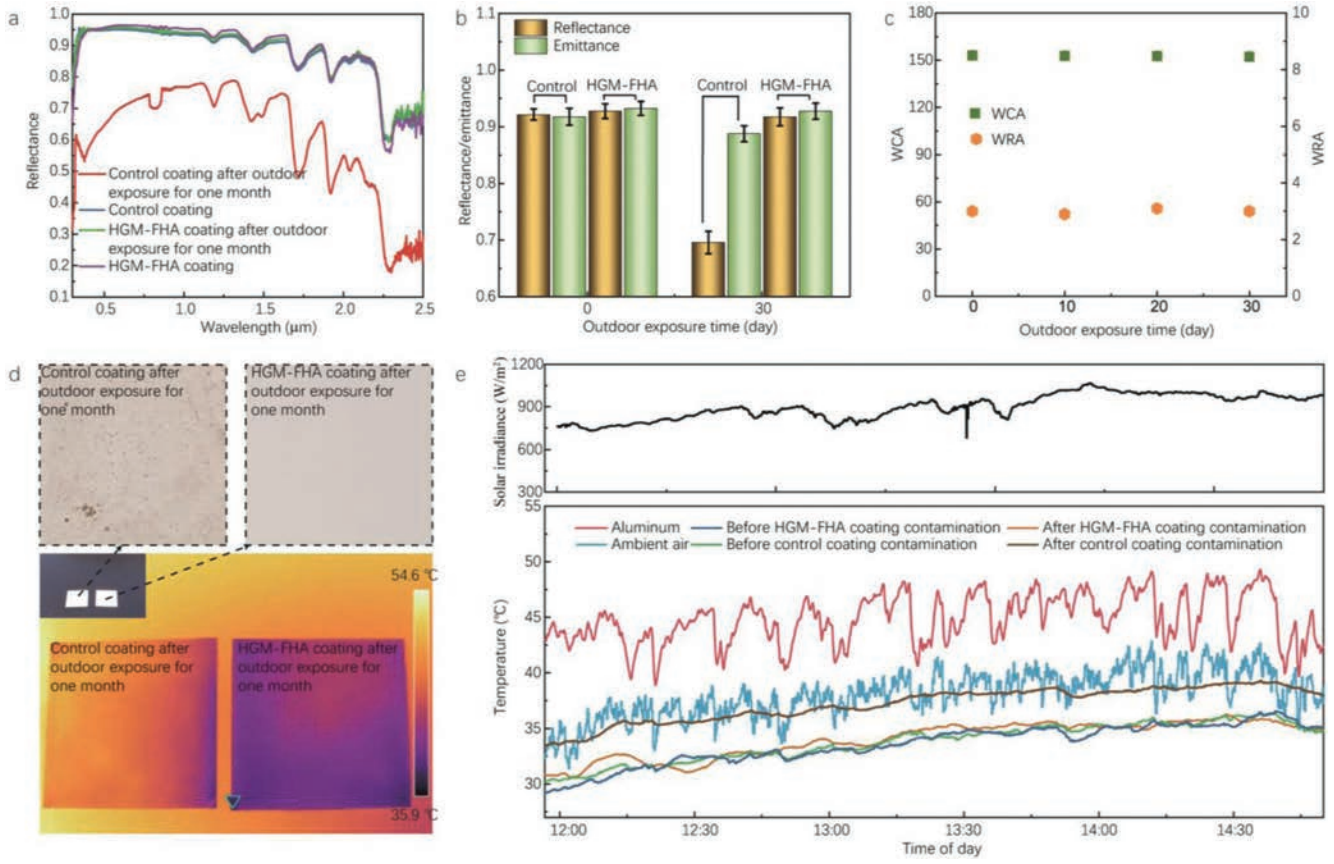

Fig. 4. The practical outdoor performance of HGM-FHA coatings. (a) The reflectance spectra of different coatings were compared to show the effect of outdoor exposure for one month. (b) Change in the average reflectance and emittance with time in outdoor exposure. (c) Change in the WCA and WRA with time in outdoor exposure. (d) The IR images and photos of coatings at 1:30 pm under direct solar radiation. (e) Temporal temperature data of the air and the hybrid coating under direct sunlight in Chengdu (date, 7 May 2022, UTC+8) and solar irradiance measured in the experiment. HGM-FHA coatings contain 80 wt% HGM with average size of ~8 μm and have thicknesses of 0.8 mm. Control coating also contain 80 wt% hollow glass beads with average size of ~8 μm and have thicknesses of 0.8 mm.

in different environments. Fig. 3e shows the adhesion strengths of the coatings on ceramic, stainless steel, aluminum, and glass. The adhesion typically exceeded 3 MPa. This firm attachment was attributed to the formation of strong covalent bonds between coatings and substrates due to abundant functional groups (-NH-CO-O-, -COO-) in the matrices (Fig. S7) [35,36]. For outdoor building applications, coating surfaces inevitably suffer from rain flushing, sun burning, and dust settling. To further evaluate the environmental stability of the coatings, we performed accelerated weathering tests based on the protocols of GB/T 9755–2014. As shown in Table S2 (Supporting information), the coatings met the standards of first-grade products, indicating their excellent practicability for use on external walls of buildings.

To further demonstrate the potential of our HGM-FHA coatings, we conducted long-time outdoor experiments. The coatings were placed outside for one month in Chengdu, China, in a humid and hot climate, using a hydrophobic coating (WCA: 109°) made from similar compositions (fluorinated hydroxy acrylic resin and hollow glass beads) as a control. The HGM-FHA coatings maintain their optical properties while the sunlight reflectance of the control was significantly reduced after one month of outdoor exposure (reduced 23%, Figs. 4a and b). The HGM-FHA coatings also retained a high WCA of >150° during the exposure period, suggesting excellent weather resistance. This stable superhydrophobicity also improved the antifouling property by making it easier to remove dust from the coating surfaces (Fig. 4c). The stable superhydrophobicity increases the antifouling property, leading to much easier removal of dust deposited on the coating surfaces by wind and rain. In contrast, the control coating was easily contaminated and showed a decrease in reflectance, resulting in lower cooling performance than the HGM-FHA coatings (Fig. 4d). The HGM-FHA coatings also had a superior self-cleaning property, as demonstrated by pouring carbon black on the coatings and observing how the water droplets cleaned the surfaces (Fig. S20 and Movie S4 in Supporting information). Outdoor tests under a condition with an average solar intensity of ~900 W/m^2, a relative humidity of ~40% at noon, and an average wind speed of ~1.0 m/s indicated that the HGM-FHA coatings could maintain an average temperature reduction of ~5 °C below the ambient under direct sunlight (Fig. 4e and Fig. S21 in Supporting information). Furthermore, in the hot summer weather (an average solar intensity of ~1000 W/m^2, a relative humidity of ~41% at noon), the HGM-FHA coatings could show the temperature reduction of ~10 °C at noon (Fig. S22 in Supporting information). This value corresponded to a theoretical net cooling power of 81.76 W/m^2 below the ambient under direct sunlight (Fig. S23 in Supporting information). Additionally, the coatings have a low thermal conductivity of 0.113 W m^{-1} K^{-1}, which helped to suppress heat exchange with the ambient atmosphere (Fig. S24 in Supporting information). In contrast, the cooling performance of the control decreased significantly after being contaminated due to its lack of efficient self-cleaning function (an average temperature elevation of ~2.6 °C was observed compared to the initial state).

In summary, we have presented a class of robust PDRC coatings with regenerable superhydrophobicity. The typical HGM-FHA coatings display a remarkable 93% sunlight reflectance and 94% mid-infrared emissivity and can effectively reduce the tempera-

ture below ambient by ~5 °C in direct sunlight. More importantly, they can regenerate their self-cleaning properties through a wear-induced reformation of superhydrophobic surfaces without any tradeoff in optical properties. We have demonstrated that this function can ensure long-lasting cooling efficiency in the outdoor environment. Since the coatings can be prepared by a simple spraying process and display good adhesion to various surfaces and excellent environmental stability, we envision their immediate application opportunities in different outdoor objects.

Declaration of competing interest

The authors declare that they have no known competing financial interests or personal relationships that could have appeared to influence the work reported in this paper.

Acknowledgments

This work was supported by the National Natural Science Foundation of China (Nos. 52003035, 52203135 and 51973023) and the CHN Energy Group Project (No. GJNY-21–183).

Supplementary materials

Supplementary material associated with this article can be found, in the online version, at doi:10.1016/j.cclet.2023.108687.

References

[1] J. Liang, J. Wu, J. Guo, et al., Nat. Sci. Rev. 10 (2022) nwac208.
[2] Z. Li, Q. Chen, Y. Song, et al., Adv. Mater. Technol. 5 (2020) 1901007.
[3] A.P. Raman, M.A. Anoma, L. Zhu, et al., Nature 515 (2014) 540–544.
[4] Y. Zhai, Y.G. Ma, S.N. David, et al., Science 355 (2017) 1062–1066.
[5] S. Zeng, S. Pian, M. Su, et al., Science 373 (2021) 692.
[6] T. Li, Y. Zhai, S. He, et al., Science 364 (2019) 760–763.
[7] B. Bhatia, A. Leroy, Y. Shen, et al., Nat. Commun. 9 (2018) 5001.
[8] D. Li, X. Liu, W. Li, et al., Nat. Nanotechnol. 16 (2021) 153.
[9] Q. Zhang, S. Wang, X. Wang, et al., Small Methods 6 (2022) 2101379.
[10] K.T. Lin, J. Han, K. Li, et al., Nano Energy 80 (2021) 105517.
[11] J. Mandal, Y. Fu, A.C. Overvig, et al., Science 362 (2018) 315–318.
[12] W. Zou, H. Luo, M. Yang, et al., Macromol. Rapid. Comm. 44 (2023) 2200695.
[13] T. Wang, Y. Wu, L. Shi, et al., Nat. Commun. 12 (2021) 365.
[14] S.H. Dong, Q. Wu, W.L. Zhang, et al., ACS Appl. Mater. Interfaces 14 (2022) 4571–4578.
[15] J. Fei, D. Han, J. Ge, et al., Adv. Funct. Mater. 32 (2022) 2203582.
[16] H.M. Zhong, Y.A. Li, P. Zhang, et al., ACS Nano 15 (2021) 10076–10083.
[17] H.X. Zhao, Q.Q. Sun, J. Zhou, et al., Adv. Mater. 32 (2020) 2000870.
[18] J. Liu, H. Tang, C. Jiang, et al., Adv. Funct. Mater. 32 (2022) 2206962.
[19] J. Zhang, C.X. Zhu, J. Lv, et al., ACS Appl. Mater. Interfaces 10 (2018) 40219–40227.
[20] K. Liu, Y. Tian, L. Jiang, Prog. Mater. Sci. 58 (2013) 503–564.
[21] F. Liu, X. Wang, M. Wang, et al., Chin. Chem. Lett. 34 (2023) 108353.
[22] X. Wang, Y. Pan, H. Yuan, et al., Chin. Chem. Lett. 31 (2020) 365–368.
[23] S. Tao, X.Y. Xu, M.X. Chen, et al., Sol. Energ. Mat. Sol. C 224 (2021) 110998.
[24] J. Wu, J. He, K. Yin, et al., Nano Lett. 21 (2021) 4209–4216.
[25] M. Chen, D. Pang, H. Yan, J. Mater. Chem. C 10 (2022) 8329–8338.
[26] C.H. Xue, R.X. Wei, X.J. Guo, et al., Compos. Sci. Technol. 220 (2022) 109279.
[27] S.J. Nie, X.Y. Tan, X.Y. Li, et al., Compos. Sci. Technol. 230 (2022) 109750.
[28] L.C. Hu, C.H. Xue, B.Y. Liu, et al., ACS Appl. Mater. Interfaces 4 (2022) 3343–3351.
[29] X.H. Liu, M.T. Zhang, Y.Z. Hou, et al., Adv. Funct. Mater. 32 (2022) 2207414.
[30] L. Liu, X.M. Shan, X.Y. Hu, et al., ACS Nano 15 (2021) 19771–19782.
[31] B.Y. Liu, C.H. Xue, H.M. Zhong, et al., J. Mater. Chem. A 9 (2021) 24276–24282.
[32] M.C. Huang, C.H. Xue, J. Huang, et al., Chem. Eng. J. 442 (2022) 136239.
[33] H. Zhang, K.C.S. Ly, X. Liu, et al., Proc. Natl. Acad. Sci. U. S. A. 117 (2020) 14657–14666.
[34] T. Wang, Y. Zhang, M. Chen, et al., Cell Rep. Phys. Sci. 3 (2022) 100782.
[35] T.J. Wood, L.J. Ward, J.P.S. Badyal, ACS Appl. Mater. Interfaces 5 (2013) 9678–9683.
[36] A. Li, Y. Jia, S. Sun, et al., ACS Appl. Mater. Interfaces 10 (2018) 10471–10479.